UDC 621.311
DOI: 10.15587/2706-5448.2025.344908

Henrikh Polshchikov,
Pavlo Zhukov

DEVELOPMENT OF A METHOD FOR MODELING THE MAGNETIC STATE AND ASSESSING THE ELECTROMECHANICAL CHARACTERISTICS OF A VORTEX LAYER OF FERROMAGNETIC PARTICLES MOVING IN A ROTATING MAGNETIC FIELD

The object of this study is a vortex layer (VL) of ferromagnetic particles (FP) moving in a rotating magnetic field (RMF). Apparatuses vortex layer (AVL) devices are used to intensify energy-intensive technological processes with liquid and bulk materials that require activation, mixing, and fine grinding. External three-phase (380 V/50 Hz) two-pole inductors are used to synthesize the VL in a cylindrical AVL working chamber with a diameter of 60–330 mm. The RMF_i modulus of magnetic induction at the bore center in the absence of FP is selected during design from the range of 0.12–0.25 T. Steel or nickel FPs have an elongated cylindrical shape, typically with a ratio of $l/d = 8–15$ (l is the FP length, d is the FP diameter) and a diameter of 0.7–2.5 mm. The magnetic and electromechanical characteristics of the VL have been insufficiently studied. This paper examines a method for estimating these characteristics of the VL by modeling its magnetic state. A real bipolar RMF existing in a working chamber with an operating VL is represented by the synchronous rotation of three plane-parallel uniform circular vector fields – field strength, induction, and magnetization $\vec{H}, \vec{B}, \vec{J}$. The experimental determination of the characteristics of the model vectors $\vec{H}, \vec{B}, \vec{J}$ is performed using two flat frame induction coils. The simple behavior patterns of the vector field are consistent with the relatively chaotic behavior of each individual VL particle.

A demonstration example of determining the characteristics of the model vectors $\vec{H}, \vec{B}, \vec{J}$, the specific torque magnetic moment, the specific power, and the level of chaos of an industrial VL is presented.

The results of this work can be used in both academic and engineering applications related to the research and design of AVL and similar equipment.

Keywords: *vortex layer in RMF, electromechanical interaction FP, magnetization model VL, optimal FP concentration, VL chaos level.*

Received: 16.09.2025
Received in revised form: 07.11.2025
Accepted: 21.11.2025
Published: 29.12.2025

How to cite
Polshchikov, H., Zhukov, P. (2025). Development of a method for modeling the magnetic state and assessing the electromechanical characteristics of a vortex layer of ferromagnetic particles moving in a rotating magnetic field. Technology Audit and Production Reserves, 6 (1 (86)), 48–56. https://doi.org/10.15587/2706-5448.2025.344908

1. Introduction

The energy of small particles with magnetic properties moving under the influence of RMF is used for various purposes. In biology and medicine, the combination of RMF and nanoscale particles gives promising results [1]. In industrial applications, FPs of micro and macro size ranges are used.

There are well-known apparatuses with a vortex layer (AVL) developed in their time, intended for the intensification of energy-consuming technological processes in liquid, gaseous, and heterogeneous media that require activation, mixing, and dispersed grinding [2]. In these devices, external three-phase (380 V/50 Hz) two-pole inductors are used for the VL synthesis in a cylindrical working chamber with a diameter of 60–330 mm. When designing inductors in the center of the working chamber in the FP absence, it is necessary to ensure the level of magnetic induction RMF_i of the order of 0.12–0.25 T.

Steel or nickel cylindrical FPs usually have a ratio of l/d = 8–15 (l – length of FP, d – diameter of FP) and a diameter of 0.7–2.5 mm, and their total volume concentration to ensure the most intensive movement, as a rule, is no more than 10% of the chamber volume.

In [2] it was shown that AVL will find application in many technological processes of the chemical, petrochemical and other industries. In [3], an extended line of these devices is presented and the use of these devices for industrial cellulose grinding and the peculiarities of their application in the food industry are discussed in detail. The devices described in [2], with some modifications, are currently manufactured by Globe Core [4]. According to the company, the requested additional areas of their application include: ecology (processing and disinfection of manure, wastewater treatment); agriculture (obtaining high-quality humus); high technologies (uranium industry, graphene production), etc. A group of Polish scientists and engineers reproduced AVL equipment in the form of a modified electromechanical mill for the mining

industry [5]. The work [6] and a systematic series of other works by these authors are devoted to the problems of cement production for the modern construction industry using VL technology. Thus, the questions of application of AVL are in dynamic development.

At the same time, the issues of electromechanics of VL, despite the fact that they are directly related to the actual practical problems of reducing energy consumption and increasing the efficiency of AVL, are insufficiently studied. There are no models that adequately describe and make it possible to predict the kinematics and dynamics of VL. In this regard, the work on creating a computer model of the electromechanical behavior of FP in VL has been started [7]. The paper [8] analytically describes the force effect of RMF on FP, but the effects of FP interaction are not investigated. In [9], the types of industrial AVL inductors were studied, analytical RMF_i calculations were carried out taking into account higher harmonics. In [10], a related design of a low-frequency mechatronic inductor for biological applications is considered. In work [11], studies of VL power were conducted and the possibility of using the field induction method for these purposes was noted, however, this idea has not been systematically developed. In [12], numerical field calculations of the RMF and characteristics of the inductor for loading with an array of parallel FPs rotating around the axial axis of the inductor were carried out. In work [13], using visual observation, cluster modes of operation of ensembles FPs were recorded under conditions not typical for classical VL.

Thus, the analysis of the existing literature shows that the general electromechanical properties of VL remain poorly studied and further scientific research in this direction is expedient. In particular, the currently unsolved problems include the study of the magnetic state of the VL and its connection with the electromechanics of the FP motion.

The object of research of this paper is the vortex layer (VL) of elongated ferromagnetic particles (FP) moving in a rotating magnetic field (RMF).

The aim of this research is the development and demonstration of a method for estimating the electromechanical characteristics of VL by modeling its magnetic state of VL.

To achieve the aim, it is necessary to solve the following tasks:

1. Develop a model of the magnetic state of the VL, a scheme for measuring model parameters and formulas for estimating the electromechanical and magnetic characteristics of the VL.
2. Conduct demonstration modeling of the magnetic state and, based on its results, determine the magnetic, energy, and structural characteristics of one of the industrial VL samples. Assess the adequacy of modeling.
3. Determine the scope of practical application of the proposed method of modeling the magnetic state and estimating the electromechanical characteristics of VL.

2. Materials and Methods

When studying the magnetic, energy, and structural state of VL, the polemetric method of studying magnetic samples of various materials was used [14]. When using this method, one coil measures the induction inside the covered sample, and the other coil measures the intensity of this field by an indirect method located outside, on the end of the sample. This method is widely used in the study of magnetic properties of materials and parts made of these materials. In electrical machines and devices, this method is also used to measure losses in electrical steel. Note that the use of the polemetric method is well-founded and studied only for elongated samples located in a longitudinal pulsating magnetic field. As for RMF, the application of this method has significant and not fully clarified features.

Features of the magnetic behavior of cylindrical samples of solid materials in a transverse magnetic field are studied in [15]. Features of the magnetic behavior and percolation magnetic effect of samples of composite materials are studied in [16]. General features of the polemetric method when measuring losses in RMF relative to electrical steels are described in [17, 18] implements modern instrumentation for such studies.

All the above-mentioned features were taken into account when developing a method for modeling the magnetic state of VL in RMF. It was considered that the VL has the shape of a finite cylinder, placed in the transverse RMF and is a composite material consisting of a liquid, gaseous or bulk matrix and ferromagnetic inclusions moving in it. The proposed method is a further development of the ideas of our earlier work [11].

An external three-phase two-pole inductor with a distributed winding was used for modeling [9]. The bore diameter of the inductor is 100 mm, the power supply is 380 V/50 Hz. RMF_i in the working chamber of the reactor in the absence of FP is practically uniform – the magnetic induction vector rotates at a frequency of 50 rps with a modulus of 0.14 T. The working chamber is non-magnetic in the form of a circular hollow cylinder made of ceramics with an internal diameter of 80 mm, equipped with thin end caps. As FP, elongated cylindrical particles made of magnetically soft spring steel wire with slightly rounded ends are used.

The induction value of the rotating magnetic field was measured by miniature coils calibrated in laboratory conditions in the field of Helmholtz coils. According to these values, the readings of the measuring frames were calibrated.

3. Results and discussion

3.1. Development of a VL magnetic state model, a model parameter measurement scheme, and formulas for estimating the VL electromechanical and magnetic characteristics

Subject and concept of modeling: VLs exhibit various rotational-oscillatory motions of FPs, including chaotic counter-impact collisions, sharp rebounds, braking, and subsequent jerks with high angular accelerations. Each FP tends to rotate around its center of mass following the induction vector, creating numerous local vortices in the process medium and inevitably leading to impact collisions of the FPs with the chamber walls and with each other. As a result, the center of mass of each particle performs chaotic translational motions throughout the chamber, reminiscent of the well-known "flea jumps" of the anchors of magnetic chemical stirrers that have become out of synchronization. The rotational motion of the particles around their centers of mass can be accompanied by intense vibration of their longitudinal axes relative to the induction vector at the frequency of a magnetic pendulum. During impact collisions and braking, magnetostrictive effects can occur, and the power density of the FP impact interaction reaches values of 10^{13} kW/m^3, with a collision rate of 10^{10} s^{-1} · m^{-3}, creating conditions for accelerating technological processes that are difficult to achieve under normal conditions [11].

Thus, the VL is a rather complex technical object. Given the random and chaotic nature of FP collisions, constructing a kinematic picture and a rigorous dynamic model of the vortex layer electromechanics seems problematic. However, experience shows that the VL enters a steady-state operating mode with a constant power consumption level within a fraction of a second after AVL startup, indicating the presence of certain regularities in its operation.

In this paper, a method for modeling the magnetic state of an industrial VL operating in an AVL with a virtually circular, uniform RMF_i is developed. Our experience shows that the circular model under consideration adequately describes the magnetic state of the VL in the working chamber of such devices and can be used to evaluate their magnetic, energy, and structural characteristics. The model can be applied to AVL with two-pole inductors and with a significant influence of higher harmonics, but the accuracy of the modeling results decreases and should be further investigated.

ISSN-L 2664-9969; E-ISSN 2706-5448

The concept of the circular model suggests an approach to studying the behavior of the VL as controlled, organized chaos, in which the instantaneous positions and instantaneous velocities of the FP are not deterministic, but the average magnetic state obeys strict and simple laws.

Preparation for modeling – ensuring a virtually uniform RMF: Assessing the degree of deviation from uniformity of the RMF in the AVL working chamber has not yet been standardized. For such an assessment, reference measurements at several characteristic points along the inductor bore can be used, either using Hall sensors [12] or miniature inductive sensors, preferably two-dimensional [9]. A simple engineering method for estimating the integral level of RMF_i heterogeneity in the area of the AVL working chamber with two-pole inductors in which the number of slots is not a multiple of four, using large-area frame coils, is shown schematically in Fig. 1.

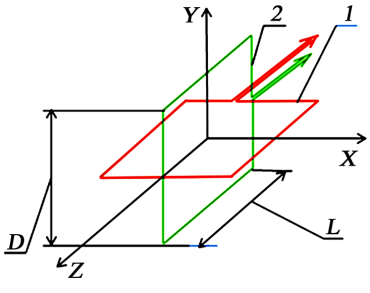

Fig. 1. Two orthogonally positioned loop coils, No. 1 and No. 2, for measuring average induction B_1 and B_2: the plane-parallel RMF_i rotates in planes perpendicular to the Z-axis, which coincides with the longitudinal axis of the inductor; D and L are the diameter and length of the cylindrical section of the inductor bore under study, with diameter D_0 and length L_0

The working chamber is located in the central region of the inductor bore, with dimensions L = 50–80% of L_0 in length and D = 80–50% of D_0 in diameter. The loop coils shown in Fig. 1 enclose the inner axial cross-section of the working chamber. This rigidly fastened pair of identical orthogonal loops can be rotated around the Z-axis. The signals from the coils are fed through integrating amplifiers either to a dual-beam oscilloscope with a time base or analyzed using Lissajous patterns. If a comparative analysis on a dual-beam oscilloscope shows that, at various fixed angles of rotation of the frames around the Z-axis, both signals are sinusoidal, have the same amplitude, and are shifted in phase by 90°, then the RMF_i region under consideration can be considered uniform and circular. If the amplitudes and/or phases of the signals differ noticeably, then this section of RMF_i is better studied using Lissajous figures. Fig. 2 shows the RMF_i Lissajous figures for various central regions of the bore of the salient-pole inductor described in [9]. A horizontal ellipse is obtained with orthogonal frames, one fixed in the plane of the tooth axis and the other in the plane of the slot axis. An inclined ellipse is obtained when the rigid system of two orthogonal frames is rotated by an angle of 45°.

Next, the VL is loaded into the chamber, and the described measurements are repeated in the same order and with the same evaluation criteria, with the only difference being that the frame coils now measure the vortex layer induction.

For AVL inductors with a multiple of four slots, it is recommended to perform diagnostic RMF scanning with a rigidly fastened pair of coils by initially positioning one frame coil in the plane of the tooth axis and the other in the plane of the slot axis, with their relative positions as close to orthogonal as possible.

The design considerations for selecting an inductor to ensure a virtually uniform circular RMF_i in the working chamber, maximally filling the inductor bore volume, were previously discussed in [9] and are not repeated here. In this study, let's use an inductor with a distributed winding and a virtually uniform circular RMF_i in the measurement chamber in the region of $L = 0.5L_0$ and $D = 0.8D_0$.

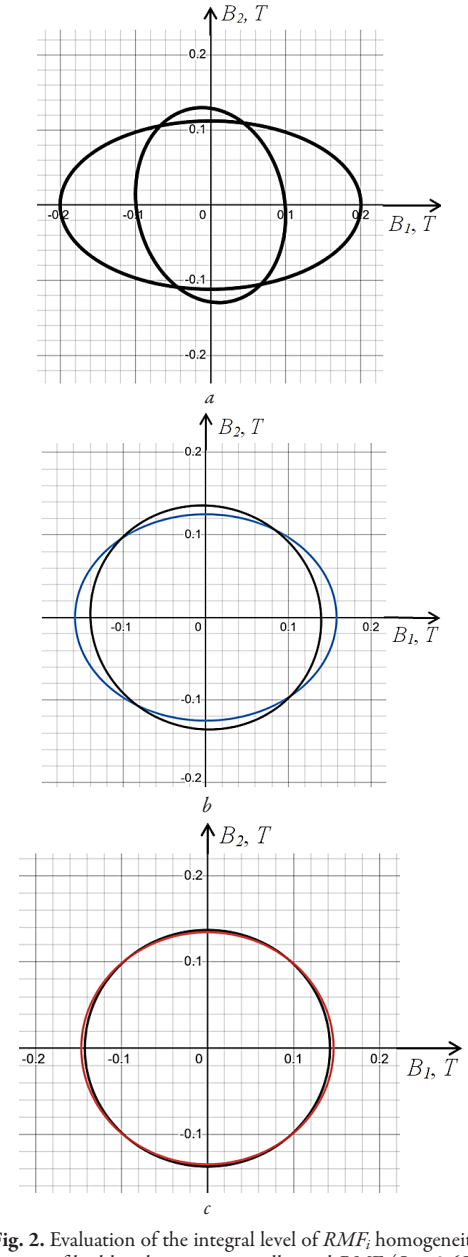

Fig. 2. Evaluation of the integral level of RMF_i homogeneity: *a* – region of highly inhomogeneous elliptical RMF_i ($L = 0.6L_0$ and $D = 0.95D_0$); *b* – region of significantly inhomogeneous field ($L = 0.6L_0$ and $D = 0.8D_0$); *c* – region of virtually uniform circular RMF_i ($L = 0.6L_0$ and $D = 0.5D_0$)

Circular model of the VL magnetic state: the actual two-pole RMF VL is modeled by three plane-parallel, uniform circular fields – field strength, magnetic induction, and magnetization $\vec{H}, \vec{B}, \vec{J}$ – rotating perpendicular to the Z-axis with constant vector modulus and the same angular velocity

$$\omega = 2\pi f, \tag{1}$$

where ω – the modulus of the angular velocity of the vector, rad/s; f – the frequency of the current in the windings of the two-pole inductor, Hz.

These three vectors are related by the fundamental vector relation of magnetic field theory for continuous media

$$\vec{B} = \mu_0 \vec{H} + \mu_0 \vec{J}, \tag{2}$$

where $\mu_0 = 4\pi 10^{-7}$ H/m.

The model of the VL circular magnetic state for each point of the working chamber is graphically depicted in Fig. 3 using a vector diagram rotating in the XY plane.

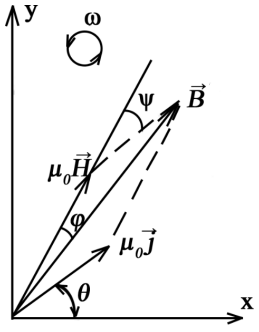

Fig. 3. Vector diagram of the VL circular magnetic state model: counterclockwise rotation; the vectors moduli and angles φ and ψ are constant; $d\theta/dt = \omega = const$

Experimental determination of vector fields characteristics $\vec{H}, \vec{B}, \vec{J}$: the experimental determination of vector fields characteristics $\vec{H}, \vec{B}, \vec{J}$ using a minimum number of sensors – one flat induction sensor and one flat field strength sensor – is shown in Fig. 4. The resulting vectors characteristics, averaged over the measurement plane, are associated with the characteristics of the model vectors $\vec{H}, \vec{B}, \vec{J}$ and extend to the entire VL volume.

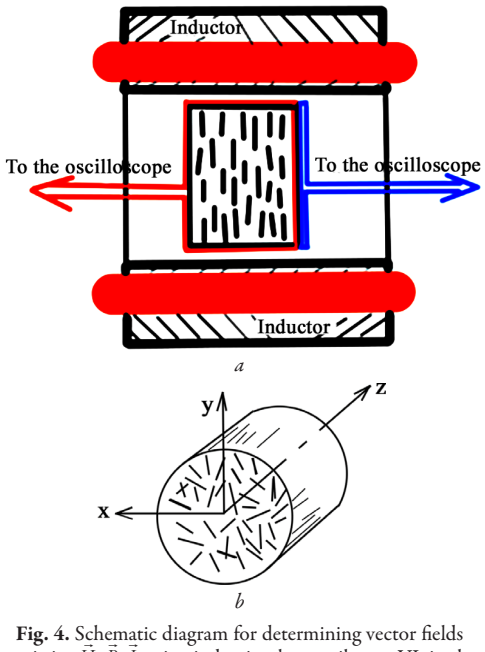

Fig. 4. Schematic diagram for determining vector fields characteristics $\vec{H}, \vec{B}, \vec{J}$ using induction loop coils: *a* – VL in the AVL working chamber; *b* – the VL cylindrical body and the location of the coordinate axes (*z* – the axial axis of the inductor)

In Fig. 4, *a*, the FPs are indicated by black dashes, the walls of the working chamber are not indicated, and the location of the induction (left sensor – red lines) and field strength (right sensor – blue lines) measuring loops is shown in a cross-section along the XZ measuring plane (top view).

The induction loop coil encloses the axial VL cross-section, while the field strength loop coil is installed in the same plane, as close to the VL end as possible and is made as narrow as possible. This shape and location of the field strength loop, in accordance with the total current law applied to an infinitely thin contour that encloses the end interface between the magnetic and non-magnetic media, allows one to obtain a volume-averaged measured field strength close to the field strength $\vec{H}$ inside VL. The frames are calculated and adjusted in the circuit connecting them to the oscilloscope plates so that the difference between their signals in a uniform RMF is zero.

The instantaneous projection values of the rotating vectors onto the measuring plane, in accordance with (2), are related by the relation

$$\mu_0 J_t = B_t - \mu_0 H_t. \quad (3)$$

Thus, by measuring the difference between the signals from the induction sensor and the field strength sensor, it is possible to experimentally determine the magnitude of the vector projection $\vec{J}$ onto the measuring plane, which let's use later.

Evaluation of the electromechanical and magnetic properties of VL – derivation of formulas for calculating the parameters.

Formulas for calculating the specific and total power VL: the specific power $P(SAR)$ of the energy RMF supplied to a unit volume of the vortex layer, or in the limit, the power density within the VL volume, as is clear from mechanics, is the scalar product of the angular velocity vector $\vec{\omega}$ (directed along the inductor axis) and the torque density vector acting on a unit volume of the vortex layer from the magnetic field

$$P(SAR) = \vec{\omega}\left(\vec{J}\times\vec{B}\right) = \vec{\omega}\left(\left(\vec{B}/\mu_0 - \vec{H}\right)\times\vec{B}\right) = \vec{\omega}\left(\vec{B}\times\vec{H}\right). \quad (4)$$

From expression (4) and the geometry of the diagram in Fig. 3, let's obtain formulas for determining the specific power VL $P_R(SAR)$, which let's use in this paper

$$P_R(SAR) = \omega JB\sin(\psi - \varphi) = \omega HB\sin\varphi = \omega\mu_0 JH\sin\psi, \quad (5)$$

where H, J, B – the vector moduli.

The first equality in expression (5) reflects the definition of the specific power in terms of the specific torque magnetic moment acting from RMF per VL volume unit. The second and third equalities in expression (5) reflect the determination of the same power through double the area of the VL elliptical "hysteresis" loop measured for the pulsating component of the uniform circular RMF.

To calculate the VL total power, the specific power is multiplied by the VL volume.

Note: it is known that two harmonic signals of the same frequency, when phase-shifted, are related by the parametric equation of an ellipse. It is easy to mathematically demonstrate that the area of the elliptical loop $B \div H$ is equal to $\pi BH\sin\varphi$, and the area of the elliptical loop $\mu_0 J \div H$ is equal to $\pi\mu_0 JH\sin\psi$.

The formula for calculating the specific torque acting within VL is: according to the physical meaning of the operating principle of the vortex layer, the force action of RMF on FP must be modeled by the torque acting on a magnetic dipole [8], that is, in the limit, by the torque density T_z in the VL volume

$$T_Z = P_R(SAR)/\omega, \quad (6)$$

where T_z – the VL specific torque, N/m^2.

This value is useful for estimating the mechanical work performed within the VL by moving FPs.

Formula for calculating the level of randomness F of FP motion in the VL: the magnetization vector field $\vec{J}$ of the vortex layer is created by the medium containing inclusions of magnetized FPs. FPs in the AVL operate in deep saturation mode even at angles of deviation of their main axis from the RMF vector of up to 70–80° [8]. The VL limiting magnetization, averaged over its volume, is obtained as

$$J_{MAX} = \frac{\delta B_s}{\mu_0}, \quad (7)$$

ISSN-L 2664-9969; E-ISSN 2706-5448

where J_{MAX} – the modulus of the VL limiting magnetization, A/m; B_s – the FP saturation induction (for steel B_s = 2 T, for nickel B_s = 0.6 T); δ – the FP volume concentration in the working chamber.

The latter is calculated using formula (8) and, for industrial VL, typically amounts to 6–8%

$$\delta = \frac{V_1 \cdot n}{V} = \frac{M}{\rho \cdot V}, \quad (8)$$

where V_1 – the volume of one FP, m^3; n – the FP number; V – the chamber volume, m^3; M – the FP total mass; ρ – the density of the FP material. To determine the concentration as a percentage, the δ value is multiplied by 100.

The VL limiting magnetization is calculated for the idealized case of a uniformly parallel arrangement of multiple FPs magnetized to saturation. For a steel FP concentration in VL equal to 0.06 (6%), the limiting value $\mu_0 J_{MAX} = \delta B_s = 0.12$ T.

The level of randomness of FP motion in VL is calculated as the difference between unity and the ratio of the modulus J of the ensemble's actual magnetization to the modulus J_{MAX} of its limiting magnetization

$$F = 1 - \frac{J}{J\max} = \frac{\mu_0 J_{MAX} - \mu_0 J}{\mu_0 J_{MAX}}, \; F\% = 100F, \quad (9)$$

where F (fan-shaped particles) – the VL chaoticity level. The chaoticity level is a structural indicator of VL and reflects the average deviation of the orientations of the FP longitudinal axes from the direction of the vector $\vec{J}$ in VL. For $J = J_{MAX}$, the longitudinal axes of all FPs are parallel to $\vec{J}$ and $F = 0$. This is the maximum level of magnetic anisotropy of the FP ensemble.

Additional magnetic parameters: VL magnetic viscosity, which characterizes, all other things being equal, the energy dissipation in VL, is determined by the rotational lag of the vectors $\vec{J}$ and $\vec{B}$ relative to the rotation of the leading vector $\vec{H}$, and can therefore be measured by angles ψ or φ.

For practical assessments and comparisons of VL response to applied RMF, scalar quantities $\mu_{VL} = B/\mu_0 H$ and $\chi_{VL} = J/H$ can be useful.

Verification of the adequacy of the proposed modeling: to verify the adequacy of the proposed model, the model measurement technology, and the calculation formulas, the VL power determined by formula (5) was compared with the reference power. The latter was measured by the difference in the values of active power consumed by the inductor at idle and operating conditions, taking into account changes in losses in its winding and steel, as described earlier in [11], taking into account the method [19].

3.2. Demonstration example of modeling the magnetic state and determining the characteristics of an industrial VL

A two-pole, three-phase inductor with a diameter and bore length of 100/120 mm, powered by a 380 V/50 Hz network, was used. The inductor, when idle, generated a nearly circular, uniform RMF_i in a working chamber with an internal diameter of 80 mm. The RMF_i induction vector uniformly rotated in a circle at a frequency of 50 rps and had a modulus B_i = 0.14 T. A process substance in gaseous, liquid, bulk, or fibrous form can be introduced into the working chamber, and then FPs made of the material under study, of the desired dimensions and concentration, can be loaded to create the VL.

Measurements are performed according to the diagram in Fig. 4, with the obtained values, averaged in the plane of the frames, distributed throughout the entire VL volume. Each measurement was repeated twice, and the numerical values obtained are presented as averages. To assess the adequacy of the obtained results, verification measurements of the VL $P_{R2}(SAR)$ power were carried out based on the difference in the active power consumed by the inductor at no-load and operating conditions, taking into account changes in losses in its winding and steel, as shown in [11, 19].

Comparative studies of different VL depending on the type and properties of the process medium, the degree of filling of the working chamber with this medium, the material and size of the FP, their concentration, the RMF characteristics, and the dimensions of the reactor working chamber are too extensive and are beyond the scope of this publication. In this paper, let's limit ourselves to presenting a demonstration example using one of the industrial VL samples. The demonstration VL sample operated in a gas environment and included a set of steel FPs with a diameter of d = 1.2 mm and a length of l = 12 mm at a concentration of δ = 0.06. The internal dimensions of the working chamber and, accordingly, the demonstration VL sample: diameter a = 80 mm, length b = 60 mm. The measurement results, averaged over the plane of the measuring frames, are presented in graphic form in Fig. 5, 6.

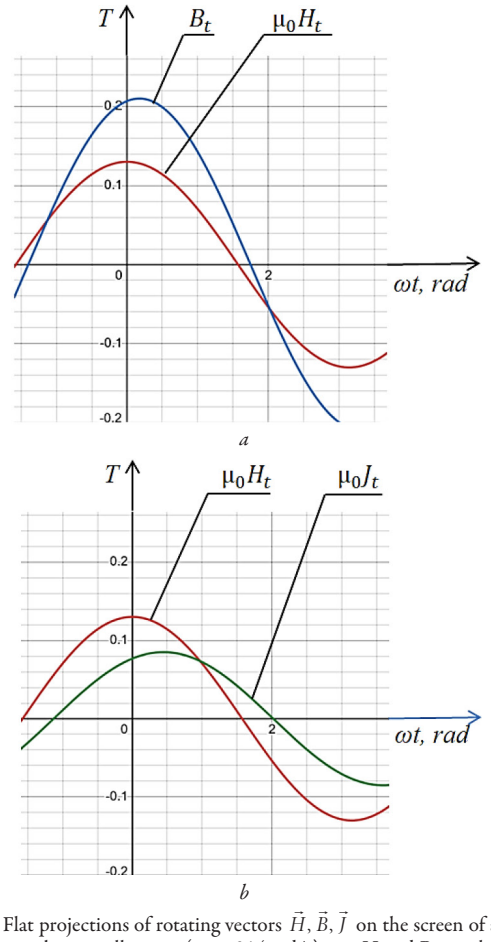

Fig. 5. Flat projections of rotating vectors $\vec{H}, \vec{B}, \vec{J}$ on the screen of a dual-beam time-base oscilloscope (ω = 314 rad/s): *a* – H and B signals: blue line – signal from the left inductor sensor $E_1 \mapsto B_t = B\cos(\omega t - \varphi)$, red line – signal from the right sensor $E_2 \mapsto \mu_0 H_t = \mu_0 H \cos(\omega t)$; *b* – H and J signals: red line – signal from the right sensor $E_2 \mapsto \mu_0 H_t = \mu_0 H \cos(\omega t)$, green line – signal difference from the two sensors, obtained experimentally when they were connected back-to-back: $(E_1 - E_2) \mapsto \mu_0 J_t = \mu_0 J \cos(\omega t - \psi)$

The signals from the sensors are integrated and amplified, and minor noise from the beats of individual FPs is filtered out. The phase shift in time between the signals from the loops is numerically equal to the angles between the rotating field vectors. The amplitudes H, B, J are numerically equal to the absolute values of the vectors $\vec{H}, \vec{B}, \vec{J}$.

Fig. 5 shows that all signals have a harmonic shape and a single frequency f. The sinusoids from the right and left sensors are shifted in time by a phase angle of $\varphi \approx 10°$, with the averaged induction amplitude B = 0.21 T and the amplitude of the signal from the right

sensor $\mu_0 H = 0.13$ T. The sine wave from the difference in the sensor signals is shifted from the sine wave of the right sensor by a phase angle of $\psi = 25°$, while the amplitude of the difference in signals $\mu_0 J = 0.085$ T.

Fig. 6 shows the elliptical parametric Lissajous loops of the VL demonstration sample for the pulsating RMF component, located perpendicular to the measurement plane. A narrow dynamic loop $B_t \div \mu_0 H_t$ was obtained by applying signals E_2 and E_1 to the horizontal and vertical plates of the oscilloscope, respectively. A wider dynamic loop $\mu_0 J_t \div \mu_0 H_t$ was obtained by applying a signal E_2 to the horizontal plates and the signal difference to the vertical plates $E_1 - E_2$. Lissajous loops provide an alternative way to determine the quantities mentioned in the previous paragraph and provide a memorable photograph of the magnetic state of the VL.

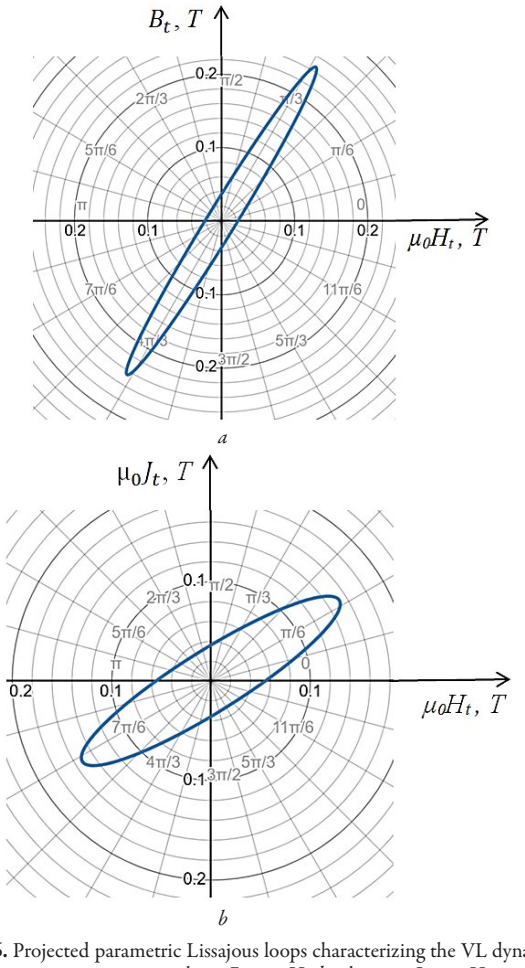

Fig. 6. Projected parametric Lissajous loops characterizing the VL dynamic magnetic state: *a* – loop $B_t \div \mu_0 H_t$; *b* – loop $\mu_0 J_t \div \mu_0 H_t$

The initial conditions, measurement results, and the absorbed power, torque parameters, chaos level, and magnetic parameters of the VL demonstration sample calculated from the simulation results are summarized in Tables 1–3.

Table 1

Measurement conditions

B_i, T	ω, rad/s	a, mm	b, mm	l/d	δ
0.14	314	80	60	12/1.2	0.06

Initial experimental conditions: is the induction modulus of a uniform RMF_i in the absence of FP in the chamber, T; ω – the angular velocity of the field rotation, rad/s; dimensions of the working chamber (VL cylindrical body): a – the diameter, mm; b – the length, mm; d, l – the diameter and length of the FP, mm; δ – the FP concentration, calculated using formula (8).

Table 2

Measurement results

B, T	$\mu_0 H$, T	φ	$\mu_0 J$, T	ψ	$P_{R2}(SAR)$, kW/dm^3
0.21	0.13	10°	0.085	25°	1.26

Results of measurements of magnetic state characteristics of VL and test power values: B – the modulus of magnetic induction $\vec{B}$ in VL, T; $\mu_0 H$ – the modulus of the vector strength $\vec{H}$ in VL multiplied by μ_0, T; $\mu_0 J$ is the modulus of the magnetization vector in VL multiplied by μ_0, T; φ, ψ – the vector shift angles according to the diagram in Fig. 3, numerically equal to the time shift angles between the corresponding measured sinusoids; $P_{R2}(SAR)$ – the specific power absorbed by VL, measured by the difference in the values of active power consumed by the inductor at no-load and operating speed, taking into account changes in losses in its winding and steel.

Table 3

Calculation results

$P_R(SAR)$, kW/dm^3	T_z, N/m^2	$\mu_0 J_{MAX}$, T	F, %	μ_{VL}	χ_{VL}
1.18	$3.7 \cdot 10^3$	0.12	29	1.6	0.65

Results of calculations of electromechanical and magnetic characteristics of VL: $P_R(SAR)$ – power absorbed by VL, calculated by formula (5) for values of H and B, H and J (the table shows the average value), kW/dm^3; $T_z = P_R(SAR)/\omega$ – specific torque calculated by formula (6), N/m^2; $\mu_0 J_{MAX}$ – value characterizing the limit magnetization of VL, calculated by formula (7), T; F% – level of VL chaos, calculated by formula (9) in %; $\mu_{VL} = B/\mu_0 H$ and $\chi_{VL} = J/H$ – conditional magnetic permeability and magnetic susceptibility of VL under conditions of magnetic anisotropy of VL.

Vector addition of magnetic moments of elongated steel particles, the major axes of which tend to be located in the direction of the magnetizing RMF, determines the resulting magnetization vector J and the level of magnetic anisotropy of VL. Moreover, the stability of the J value has been confirmed experimentally, thereby confirming the concept of the VL structure as a stable, organized chaos; the values of J, H, and B change only with FP wear.

Table 3 shows, using the values μ_{VL} and χ_{VL}, that the VL with a 94% gas filler is quite actively magnetized under the RMF conditions under consideration. This conclusion also applies to VLs operating with liquid or bulk fillers.

The significant level of chaos – $F = 29\%$ – indicates that the FPs in the VL operate in a high-intensity impact collision mode with the destruction of cluster nuclei. Indeed, high-speed video footage of the studied VL consistently shows a significant spread in the chaotically changing orientations of the long axes of the moving working particles; no stable clusters are observed.

The magnetic viscosity and power consumption of this VL, operating in air at atmospheric pressure, are also high. Angle $\psi = 25°$; $P_R(SAR) = 1.18$ kW/dm^3.

The agreement between the value $P_R(SAR)$ and the verified power measurement (Table 2) is satisfactory, indicating the adequacy of the proposed model, measurement technology, and calculation formulas.

Thus, it has been experimentally confirmed that, despite the non-deterministic position and instantaneous velocity of each FP, the proposed simple circular model can be successfully applied to the description and calculation of the magnetic and electromechanical characteristics of the VL. In this model, the VL magnetization vector

ISSN-L 2664-9969; E-ISSN 2706-5448

is constant in magnitude and rotates at a constant angular velocity, synchronously lagging the magnetizing vector RMF by a constant phase angle. Using the characteristics of the introduced model vectors, it is possible to quickly and accurately estimate the following parameters important for practical applications:

– VL electromechanical parameters: its specific and total power, specific torque, and the degree of randomness of the FP motion;
– VL magnetic parameters: conditional magnetic permeability and conditional magnetic susceptibility VL under conditions of VL magnetic anisotropy.

3.3. Practical application of the developed method for modeling the magnetic state and assessing the VL electromechanical characteristics

In general, the research results demonstrate that a VL is a system of low-inertia FPs that, under the RMF influence, almost instantly enters a steady-state operating mode characterized by long-term stability and simple behavioral patterns of the average magnetization vector $\vec{J}$, despite the non-deterministic position and instantaneous velocity of each FP. Thus, a VL demonstrates an example of controlled organized chaos and should be further described in this light. The established ability to obtain the considered set of experimental data for any specific vortex layer provides a platform for:

– comparing the characteristics of different VLs operating under various conditions and environments;
– more detailed identification of the forms and types of mechanical motion of FPs operating in the organized chaos mode, responsible for ensuring VL operation according to the established patterns;
– developing and improving predictive electromechanical models of VLs, including using computer simulation;
– obtaining input data for AVL design programs, in particular for computer calculations of inductors operating with VL.

Let's briefly consider the latter issue. When calculating inductors for AVL operating with VL, knowledge of the magnetic characteristics of the latter is required. Table 4 provides comparative data on some magnetic and structural characteristics of VL for the model proposed in [12] (MSH indices) and the model proposed in this paper (PG indices).

Table 4

Comparative magnetic and structural characteristics of VL

MSH			PG		
μ_{rd}	F%	β	μ_J	F%	ψ
10	≈0	<33°	1.72	29	25°

In Table 4: μ_{rd} – the relative magnetic permeability of the FP ensemble, calculated in the MSH model in Cartesian coordinates d, q along the d-axis directed along the orientation line of the major axis of the parallel FPs; F% – the VL chaos level; β – the angle between the magnetomotive force vector and the d-axis during stable operation of the inductor under load; μ_J – the ratio of the projections of the vectors $\vec{B}$ and $\mu_0\vec{H}$ onto the direction of the vector $\vec{J}$; ψ – the angle between the vectors $\vec{H}$ and $\vec{J}$ in the PG model (almost corresponds to the angle β in the MSH model).

A comparison of the data shows that the value of μ_{rd}, which is the base value for calculating the inductor characteristics under load in the MSH model, is significantly overestimated compared to a similar value μ_J established through physical modeling. This discrepancy can be partially explained by the following factors:

– the MSH model studies an ensemble of FPs in the form of an array of parallel particles ($F \approx 0$) rotating in the working chamber around the axial axis of the inductor. Such FP behavior, as demonstrated above, is atypical for industrial AVLs and overestimates the average magnetization and magnetic field induction inside the VL;
– the MSH mathematical model considers excessively dense FP packing. It is necessary to take into account that when FPs are loaded into the working chamber in excessive quantities, the intensity of their motion decreases, and ultimately the FPs magnetically adhere to each other and aggregate into solid structures, the formation of which results in the VL ceasing to exist, as shown in monograph [2] and in Fig. 7. Due to significant friction against the inner surface of the chamber, these structures can be stationary or rotate, usually at a speed significantly lower than ω, around the axial axis of the inductor. The magnetic state and electromechanical characteristics of such pseudo-solid formations are not described by the circular model and are not considered in this paper.

To ensure the most intense FP movement in the working chamber, industrial AVLs use optimal volume concentrations δ, determined experimentally for specific conditions and typically not exceeding 10%.

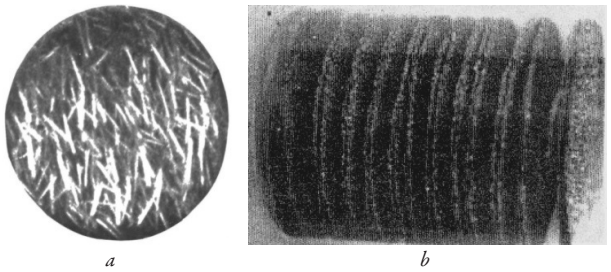

a *b*

Fig. 7. Phase states of an FP ensemble in a cylindrical AVL working chamber at different particle volume concentrations [3]: *a* – vortex layer of rapidly moving elongated FPs (particle concentration 6–8%), high-speed filming of VL operation from the end of the inductor at 1000 fps; *b* – parallel disks formed by closely packed, linked FPs (particle concentration above 12%), profile shot

In any case, there is a clear need to work towards reconciling the VL models implemented in various studies. Moreover, to refine estimates of the magnetic and electromechanical state of VL when calculating the characteristics of AVL inductors operating under load, it is advisable to rely on the results of VL physical modeling similar to that described in this paper. This will significantly bring the calculated characteristics closer to industrial practice of VL use.

Limitations – if the VL operating conditions deviate significantly from those described in this paper, the accuracy of the estimates decreases and should be further investigated.

In the future, it would be useful to use the results of this work for comparative studies and predictions of VL behavior under various operating conditions, as well as in the AVL design process. It would also be of interest to explore alternative methods for determining characteristics $\vec{H}$ applicable to VL.

4. Conclusions

1. In this study, a model of the magnetic state is developed, a scheme for measuring the model parameters is proposed, and formulas are derived for estimating the magnetic and electromechanical characteristics of a VL operating in a long-term stable mode. A concept is used that assumes an approach to studying the VL behavior as a controlled organized chaos in which instantaneous positions and instantaneous FP speeds are not deterministic, but the average magnetic state obeys strict and simple laws. A real bipolar RMF existing in the working chamber with an operating VL is represented in the model by synchronous rotation of three plane-parallel homogeneous circular vector fields – field strength, induction, and magnetization $\vec{H}, \vec{B}, \vec{J}$. Experimental determination of the characteristics of the model vectors

$\vec{H}, \vec{B}, \vec{J}$ is performed using two flat frame induction coils according to a special scheme. Simple and convenient for practical use formulas for calculating the electromechanical and magnetic characteristics of VL are derived and substantiated: specific and total power; specific torque magnetic moment; level of chaos of FP motion. The conditional magnetic permeability and conditional magnetic susceptibility of the VL under magnetic anisotropy conditions were determined. The applicability limits of the method were determined.

2. A demonstration simulation of the magnetic state was conducted, and the magnetic and electromechanical characteristics of an industrial VL were determined using its results. It was experimentally confirmed that the VL operates in an organized chaos mode: the instantaneous position and instantaneous velocity of each FP are not determined, but the behavior of the vectors $\vec{H}, \vec{B}, \vec{J}$ obeys a circular law. All vectors rotate with a phase shift at a constant angular velocity ω equal to the rotational speed of the inductor's magnetic field vector. With the magnitude of the inductor's external field vector equal to 0.13 T, the resulting induction vector VL has a magnitude of 0.21 T. During rotation, the magnetization vector VL lags behind the inductor's magnetic field vector by a constant phase angle determined by the magnetic viscosity of VL within 25°. The modulus of the magnetization vector VL operating in a gas environment is constant and amounts to 71% of the maximum possible magnetization of VL. Based on the measurement results, the electromechanical and magnetic parameters of VL were calculated: specific power – 1.18 kW/dm^3; specific torque – 3.7×10^3 N/m^2; randomness level of FP motion – 29%; conditional magnetic permeability – 1.6; conditional magnetic susceptibility – 0.65.

Comparison with the VL power value determined by an alternative method confirmed the adequacy of the proposed model, measurement technology, and calculation formulas.

3. The proposed method is further recommended for:

– modeling and comparing the characteristics of various VLs operating in different conditions and environments;

– a more detailed identification of the forms and types of mechanical motion of low-inertia FPs operating in organized chaos mode, responsible for ensuring stable operation of the VL according to established patterns;

– development of predictive electromechanical models of the VL using computer simulation to identify the parameters of the fan-shaped deviation of the FPs major axes from the direction of the vector $\vec{J}$;

– obtaining input data for AVL design programs and computer calculations of inductors in their VL mode, which should be based on the characteristics of model circular vectors.

Conflict of interest

The authors declare that they have no conflict of interest in relation to this research, whether financial, personal, authorship or otherwise, that could affect the research and its results presented in this paper.

Financing

The research was performed without financial support.

Data availability

The manuscript has no associated data.

Use of artificial intelligence

The authors confirm that they did not use artificial intelligence technologies when creating the current work.

Authors' contributions

Henrikh Polshchikov: Conceptualization, Methodology, Investigation, Writing – original draft, Writing – review and editing; ***Pavlo Zhukov***: Conceptualization, Methodology, Investigation, Writing – original draft, Writing – review and editing.

References

1. Moerland, C. P., van IJzendoorn, L. J., Prins, M. W. J. (2019). Rotating magnetic particles for lab-on-chip applications – a comprehensive review. *Lab on a Chip, 19 (6),* 919–933. https://doi.org/10.1039/c8lc01323c
2. Logvinenko, D. D., Sheliakov, O. P. (1976). *Intensifikatciia tekhnologicheskikh protcessov v apparatakh s vikhrevym sloem.* Kyiv: Tekhnika, 144.
3. Oberemok, V. M. (2010). *Elektromahnitni aparaty z feromahnitnymy robochymy elementamy. Osoblyvosti zastosuvannia.* Poltava: RVV PUSKU, 201. Available at: http://dspace.puet.edu.ua/handle/123456789/6536
4. *GlobeCore Transformer Oil Purification Equipment, Bitumen Equipment.* Available at: https://globecore.com/ Last accessed: 22.09.2023
5. Ogonowski, S. (2021). On-Line Optimization of Energy Consumption in Electromagnetic Mill Installation. *Energies, 14 (9),* 2380. https://doi.org/10.3390/en14092380
6. Ibragimov, R., Korolev, E., Potapova, L., Deberdeev, T., Khasanov, A. (2022). The Influence of Physical Activation of Portland Cement in the Electromagnetic Vortex Layer on the Structure Formation of Cement Stone: The Effect of Extended Storage Period and Carbon Nanotubes Modification. *Buildings, 12 (6),* 711. https://doi.org/10.3390/buildings12060711
7. Calus, D. (2023). Experimental Research into the Efficiency of an Electromagnetic Mill. *Applied Sciences, 13 (15),* 8717. https://doi.org/10.3390/app13158717
8. Polshchikov, H., Zhukov, P. (2023). Force effect of a circular rotating magnetic field of a cylindrical electric inductor on a ferromagnetic particle in process reactors. *Technology Audit and Production Reserves, 6 (1 (74)),* 34–40. https://doi.org/10.15587/2706-5448.2023.293005
9. Polshchikov, H., Zhukov, P. (2024). Construction of a generalized mathematical model and fast calculations of plane-parallel rotating magnetic fields in process reactors with longitudinal currents of cylindrical inductors on a graphical calculator. *Technology Audit and Production Reserves, 5 (1 (79)),* 38–49. https://doi.org/10.15587/2706-5448.2024.313937
10. Hallali, N., Rocacher, T., Crouzet, C., Béard, J., Douard, T., Khalfaoui, A. et al. (2022). Low-frequency rotating and alternating magnetic field generators for biological applications: Design details of home-made setups. *Journal of Magnetism and Magnetic Materials, 564,* 170093. https://doi.org/10.1016/j.jmmm.2022.170093
11. Polshchikov, G. A., Logvinenko, D. D., Zhukov, P. B. (1975). Nekotorye voprosy rascheta i proektirovaniia apparatov s vikhrevym sloem, NIIKhIMMASh. *Oborudovanie s ispolzovaniem razlichnykh metodov intensifikatcii protcessov, 71,* 128–141.
12. Milykh, V. I., Shilkova, L. V. (2020). Characteristics of a cylindrical inductor of a rotating magnetic field for technological purposes when it is powered from the mains at a given voltage. *Electrical Engineering & Electromechanics, 2,* 13–19. https://doi.org/10.20998/2074-272x.2020.2.02
13. Milykh, V. I., Shylkova, L. V. (2020). Experimental research of the three-phase physical model of the magnetic field inductor in the working mode when processing bulk material. *Bulletin of NTU "Kharkiv Polytechnic Institute" Series: Electrical Machines and Electromechanical Energy Conversion, 3 (1357),* 3–7. https://doi.org/10.20998/2409-9295.2020.3.01
14. Guo, Y., Zhu, J. G., Zhong, J., Lu, H., Jin, J. X. (2008). Measurement and Modeling of Rotational Core Losses of Soft Magnetic Materials Used in Electrical Machines: A Review. *IEEE Transactions on Magnetics, 44 (2),* 279–291. https://doi.org/10.1109/tmag.2007.911250
15. Prozorov, R., Kogan, V. G. (2018). Effective Demagnetizing Factors of Diamagnetic Samples of Various Shapes. *Physical Review Applied, 10 (1).* https://doi.org/10.1103/physrevapplied.10.014030
16. Mattei, J.-L., Floc'h, M. L. (2003). Percolative behaviour and demagnetizing effects in disordered heterostructures. *Journal of Magnetism and Magnetic Materials, 257 (2-3),* 335–345. https://doi.org/10.1016/s0304-8853(02)01232-5
17. Atallah, K., Howe, D. (1993). Calculation of the rotational power loss in electrical steel laminations from measured H and B. *IEEE Transactions on Magnetics, 29 (6),* 3547–3549. https://doi.org/10.1109/20.281225

ISSN-L 2664-9969; E-ISSN 2706-5448

18. Alatawneh, N., Pillay, P. (2011). Design of a novel test fixture to measure rotational core losses in machine laminations. *2011 IEEE Energy Conversion Congress and Exposition.* Phoenix, 433–440. https://doi.org/10.1109/ecce.2011.6063802

19. Polshchikov, G. A., Zhukov, P. B. (1978). A.Cv. na izobretenie SU 627848 A1. *Sposob kontrolia protcessov v apparate s vikhrevym sloem.* Published: 15.10.78, Bul. No. 38.

✉***Henrikh Polshchikov,*** *Head of the Electromagnetic Devices Sector (retired), Department of Vortex Mixing Apparatus, Private Joint Stock Company "Research and Development Institute of Enameled Chemical Equipment and New Technologies Kolan", Poltava, Ukraine, e-mail: genrikharonovich@gmail.com, ORCID: https://orcid.org/0009-0001-2197-2373*

Pavlo Zhukov, *Electrician Engineer (retired), Private Joint Stock Company "Research and Development Institute of Enameled Chemical Equipment and New Technologies Kolan", Poltava, Ukraine, ORCID: https://orcid.org/0009-0005-5661-0275*

✉*Corresponding author*